

# Multi-variate probability density functions with dynamics for cloud droplet activation in large-scale models: single column tests

H. Guo<sup>1</sup>, J.-C. Golaz<sup>2</sup>, L. J. Donner<sup>2</sup>, V. E. Larson<sup>3</sup>, D. P. Schanen<sup>3</sup>, and B. M. Griffin<sup>3</sup>

<sup>1</sup>UCAR Visiting Scientist Programs, NOAA/Geophysical Fluid Dynamics Laboratory, Princeton, NJ, USA

<sup>2</sup>NOAA/Geophysical Fluid Dynamics Laboratory, Princeton, NJ, USA

<sup>3</sup>University of Wisconsin-Milwaukee, Milwaukee, WI, USA

Received: 27 April 2010 – Published in Geosci. Model Dev. Discuss.: 11 May 2010

Revised: 30 August 2010 – Accepted: 22 September 2010 – Published: 8 October 2010

**Abstract.** Successful simulation of cloud-aerosol interactions (indirect aerosol effects) in climate models requires relating grid-scale aerosol, dynamic, and thermodynamic fields to small-scale processes like aerosol activation. A turbulence and cloud parameterization, based on multi-variate probability density functions of sub-grid vertical velocity, temperature, and moisture, has been extended to treat aerosol activation. Multi-variate probability density functions with dynamics (MVD PDFs) offer a solution to the problem of the gap between the resolution of climate models and the scales relevant for aerosol activation and a means to overcome the limitations of diagnostic estimates of cloud droplet number concentration based only on aerosol concentration.

Incorporated into the single-column version of GFDL AM3, the MVD PDFs successfully simulate cloud properties including precipitation for cumulus, stratocumulus, and cumulus-under-stratocumulus. The extension to treat aerosol activation predicts droplet number concentrations in good agreement with large eddy simulations (LES). The droplet number concentrations from the MVD PDFs match LES results more closely than diagnostic relationships between aerosol concentration and droplet concentration.

In the single-column model simulations, as aerosol concentration increases, droplet concentration increases, precipitation decreases, but liquid water path can increase or decrease.

## 1 Introduction

The diversity of climate sensitivity among current model projections is explained in part by low-level clouds, and models probably fail to include processes which could introduce further uncertainty (Webb et al., 2006; Forster et al., 2007). Cloud-aerosol interactions are an important aspect of the role of low clouds in climate sensitivity (Heintzenberg and Charlson, 2009), and are also a major source of uncertainty in climate projections (Kiehl, 2007).

A key bridge between clouds and aerosols is aerosol activation. Aerosol activation depends on local super-saturation and hence vertical velocity at scales far below those resolved in climate models with horizontal spacing of  $\sim 100$  km. Due to the significant sub-grid variability in vertical velocity (Leary and Houze, 1980; Donner et al., 1999; Stevens et al., 2005) and the nonlinear dependence of aerosol activation on vertical velocity, using average fields at the coarse resolution of climate models for aerosol activation is highly problematic.

In face of these conceptual difficulties, we have adopted a multi-variate probability density function approach to represent the sub-grid variations in vertical velocity, liquid water potential temperature, and total water content in a model grid box (Golaz et al., 2002a, b, 2007; Larson et al., 2002; Larson and Golaz, 2005). Although probability density functions (PDFs) representing sub-grid variations in moisture and/or temperature have been employed in the past for the parameterization of fractional cloudiness (Mellor, 1977), parameterizations that include joint variations in vertical velocity are rare (Lappen and Randall, 2001). The inclusion of vertical velocity can not only predict sub-grid variations in vertical velocity required by aerosol activation, but also



Correspondence to: H. Guo  
(huan.guo@noaa.gov)

combine this dynamic variability with thermodynamic variability (e.g., temperature and moisture) in a self-consistent fashion.

Multi-variate probability density functions with dynamics (MVD PDFs) are a potential solution to the problem of the gap between the resolution of climate models and the scales relevant for aerosol activation. The main purpose of this paper is to link aerosol activation to the MVD PDFs. In addition to using the PDF of vertical velocity directly for aerosol activation, we further incorporate the turbulent transport of cloud droplet number concentration ( $N_d$ ) and couple with a two-moment microphysics scheme (Morrison and Gettelman, 2008; Salzmann et al., 2010).  $N_d$  is predicted via a budget equation (Ghan et al., 1997; Lohmann et al., 1999; Ming et al., 2007; Morrison and Gettelman, 2008).

This paper evaluates the performance of the MVD PDFs in the framework of the single column model (SCM) of GFDL atmospheric general circulation model (AM3) (Donner et al., 2010), because the SCM configuration is an efficient framework for implementing and performing the initial evaluations of new physical packages and avoids the complexity of a full general circulation model (GCM) (Randall et al., 1996). The source code for the MVD PDFs is referred to as CLUBB (Cloud Layers Unified By Binormals) (<http://clubb.larson-group.com>). We interfaced the GFDL SCM to CLUBB, and hereafter refer to it as GFDL SCM-CLUBB. Our main goals are twofold: (1) to improve simulations of boundary layer and associated clouds in the GFDL SCM through the use of the MVD PDFs, and (2) to extend the MVD PDFs to activate aerosols. The latter is a novel application of the MVD PDFs, whose success is critical for its use in parameterizing aerosol-cloud interactions in GCMs.

The paper is organized as follows. Section 2 describes the incorporation of the prognostic treatment of cloud droplet number concentration and microphysics. Section 3 shows simulations of representative cloud cases and evaluates them against large eddy simulations (LES) and available observations. Section 4 provides conclusions. The appendix presents lower resolution simulations.

## 2 Prognostic equation for droplet number concentration

The MVD PDFs are unique in that they predict the joint distribution of temperature, water mass, and vertical velocity. The distribution of vertical velocity is then a natural link to aerosol activation. So the MVD PDFs have precisely the information needed to consistently diagnose the activation. The significance of sub-grid variation of vertical velocity is evident, especially when the grid mean vertical velocity is negative or zero, but both small-scale upward and downward motions are present. For example, stratocumulus regimes occur in environments of large-scale subsidence, but only small-scale updrafts activate cloud droplets.

The GFDL AM3 has incorporated a mechanistic aerosol activation scheme developed by Ming et al. (2006), which diagnoses the concentration of activated droplet numbers  $N_{act}(w)$  as a function of vertical velocity  $w$  and aerosol characteristics and concentration. The aerosol activation scheme provides an initial cloud droplet number concentration. Cloud droplets are also subject to turbulent transport and/or mixing, evaporation, collision and/or coalescence, and other physical processes. To explore the effects of aerosols on low-level clouds, we have further incorporated the treatment of turbulent transport and/or mixing of the cloud droplet number concentration, and coupled with two-moment microphysics. The prognostic equation for the droplet number concentration is as follows:

$$\frac{\partial \overline{N_d}}{\partial t} = -\overline{w} \frac{\partial \overline{N_d}}{\partial z} - \frac{\partial}{\partial z} \overline{w' N_d'} + S - A - C - E \quad (1)$$

where  $\overline{N_d}$  is the layer-averaged droplet number concentration,  $\overline{w} \frac{\partial \overline{N_d}}{\partial z}$  is the large-scale transport of cloud droplets and  $\overline{w}$  is an imposed large-scale vertical velocity,  $\frac{\partial}{\partial z} \overline{w' N_d'}$  is the turbulent transport of cloud droplets (Ovchinnikov and Ghan, 2005),  $S$  denotes a droplet source term due to aerosol activation, and  $A$ ,  $C$ , and  $E$  denote droplet sink terms due to autoconversion, collection by rain, and evaporation, respectively.

A droplet source term due to aerosol activation,  $S$ , is expressed as the difference between number concentration of droplets that can be activated and pre-existing droplet number concentration (Stevens et al., 1996; Ghan et al., 1997; Lohmann et al., 1999), that is,

$$S = \max(\overline{N_{act}} - \overline{N_d}, 0) / \Delta t \quad (2)$$

where  $\Delta t$  is the host SCM time step, and  $\overline{N_{act}}$  is the layer-averaged droplet number concentration due to the activation process. For pre-existing clouds, new droplets form if the number of activated droplets,  $\overline{N_{act}}$ , exceeds the existing droplets  $\overline{N_d}$ .

Since the activation process occurs only within saturated updrafts, and since the saturation (i.e., cloudiness) can be diagnosed based on the PDF of liquid potential temperature ( $\theta_l$ ) and total water content ( $q_t$ ) for clouds, we integrate over the joint PDF to calculate  $\overline{N_{act}}$ , i.e.,

$$\overline{N_{act}} = \int_w \int_{\theta_l} \int_{q_t} N_{act}(w) \text{PDF}(w > 0, \text{CF}(\theta_l, q_t) > 0) dw d\theta_l dq_t \quad (3)$$

The numerical integration of Eq. (3) is performed using a 196-point Gauss-Hermite quadrature for each of the Gaussians in the underlying joint PDF. In addition to  $\overline{N_{act}}$ , information on the PDF of  $N_{act}$  remains available (Sect. 3.3). Note that  $\overline{N_{act}}$  is an areal average and does not imply that droplets are uniformly distributed horizontally. In general, it will be used in a large-scale model in a way that takes account of

sub-grid variability, e.g., by applying to cloudy regions after normalizing by cloud fraction, sub-columns (Pincus et al., 2006), or Latin hyper-cube sampling (Larson et al., 2005).

Cloud droplet sinks due to autoconversion ( $A$ ) and collection ( $C$ ) are assumed to be linearly proportional to warm cloud mass sinks due to the corresponding processes (Morrison and Gettelman, 2008). Evaporation,  $E$ , is assumed to be linearly proportional to the changes in cloud fraction (CF) as follows:

$$A = -\min\left(\frac{\overline{N_d}}{q_c} \left(\frac{\Delta q_c}{\Delta t}\right)_{\text{auto}}, 0\right) \quad (4)$$

$$C = -\min\left(\frac{\overline{N_d}}{q_c} \left(\frac{\Delta q_c}{\Delta t}\right)_{\text{accr}}, 0\right) \quad (5)$$

$$E = -\min\left(\frac{\overline{N_d}}{\text{CF}} \frac{\Delta \text{CF}}{\Delta t}, 0\right). \quad (6)$$

Morrison and Gettelman (2008) two-moment microphysics is applied to temperature, moisture, and cloud droplet concentrations averaged over the cloudy portion of the MVD PDFs (e.g., Eq. 3). The vertical spacing is  $\sim 40$  m in the lowest 2 km of the atmosphere (Fig. A1), and there are 101 vertical levels from the surface to the top of the atmosphere ( $\sim 40$  km). The time steps are 3 min for both the MVD PDFs and the host SCM. Note that the effects of reducing resolution are discussed in the Appendix.

### 3 Simulation results

To a large extent, boundary layer moist convection can be divided into three main regimes: a deep planetary boundary layer with a small cloud fraction capped by a weak inversion, a shallow planetary boundary layer with a high cloud fraction capped by a strong inversion, and an intermediate one (Stevens et al., 2001). Here we show simulations corresponding to these representative regimes. We select cloud cases that have been studied by the Global Energy and Water Exchange Cloud System Study (GCSS) Boundary Layer Cloud Working Group (BLCWG). They are well-established benchmarks to evaluate parameterizations and cloud models.

We have investigated three observationally non-precipitating cases:

- a trade-wind cumulus case during the Barbados Oceanographic and Meteorological Experiment (BOMEX) (Siebesma, et al., 2003),
- a non-drizzling marine stratocumulus case during the First Research Flight (RF01) of the Second Dynamics and Chemistry of Marine Stratocumulus Field Study (DYCOMS-II) (Stevens et al., 2005),
- a cumulus-under-stratocumulus case during the Atlantic Trade Wind Experiment (ATEX) (Stevens et al., 2001),

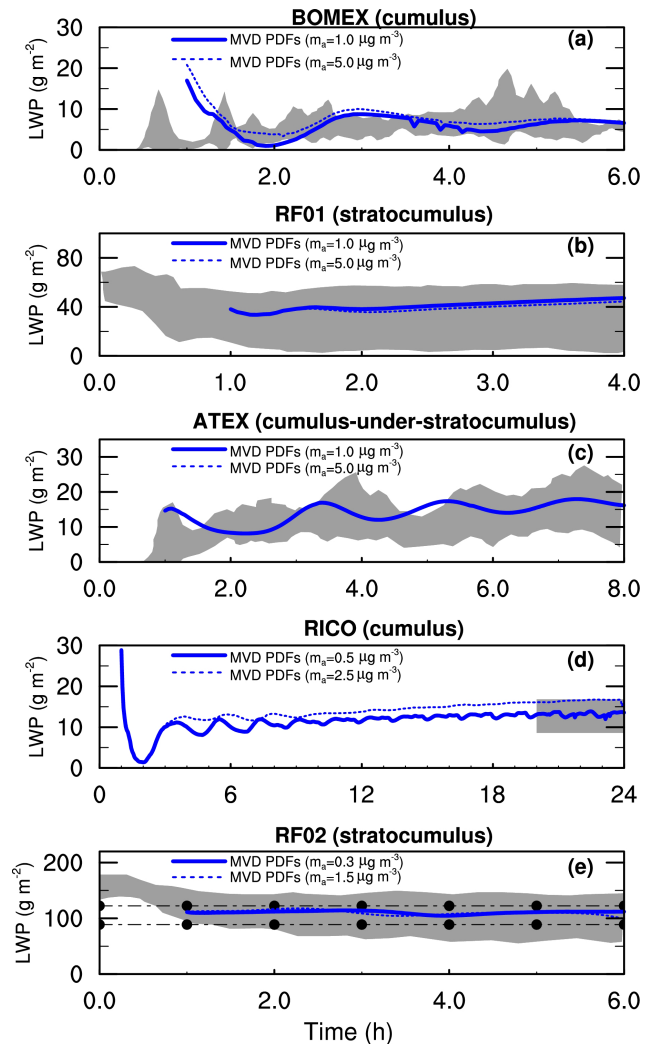


**Fig. 1.** Time series of liquid water path (LWP) for BOMEX in (a), RF01 in (b), ATEX in (c), RICO in (d), and RF02 in (e) at different sulfate aerosol mass concentrations ( $m_a$ ). The time series from the MVD PDFs begin from the first hour when microphysics is activated. The solid and dotted curves are overlapped in (c) because the changes in LWP are small when  $m_a$  increases from 1.0 to  $5.0 \mu\text{g m}^{-3}$  in ATEX. Shaded areas in (a), (b), (c), and (e) indicate the ranges of the LES ensemble. The shaded area in (d) indicates the LWP ranges of S-S LES averaged over the last 4 h. Dots in (e) indicate approximate measurement ranges for RF02 (Stevens et al., 2003).

and two observationally precipitating cases:

- the Rain In Cumulus over the Ocean (RICO) (Stevens and Seifert, 2008),
- the Second Research Flight (RF02) of DYCOMS-II (Ackerman et al., 2009).

The entire simulation periods for BOMEX, RF01, ATEX, RICO, and RF02 are 6 h, 4 h, 8 h, 24 h, and 6 h, respectively.

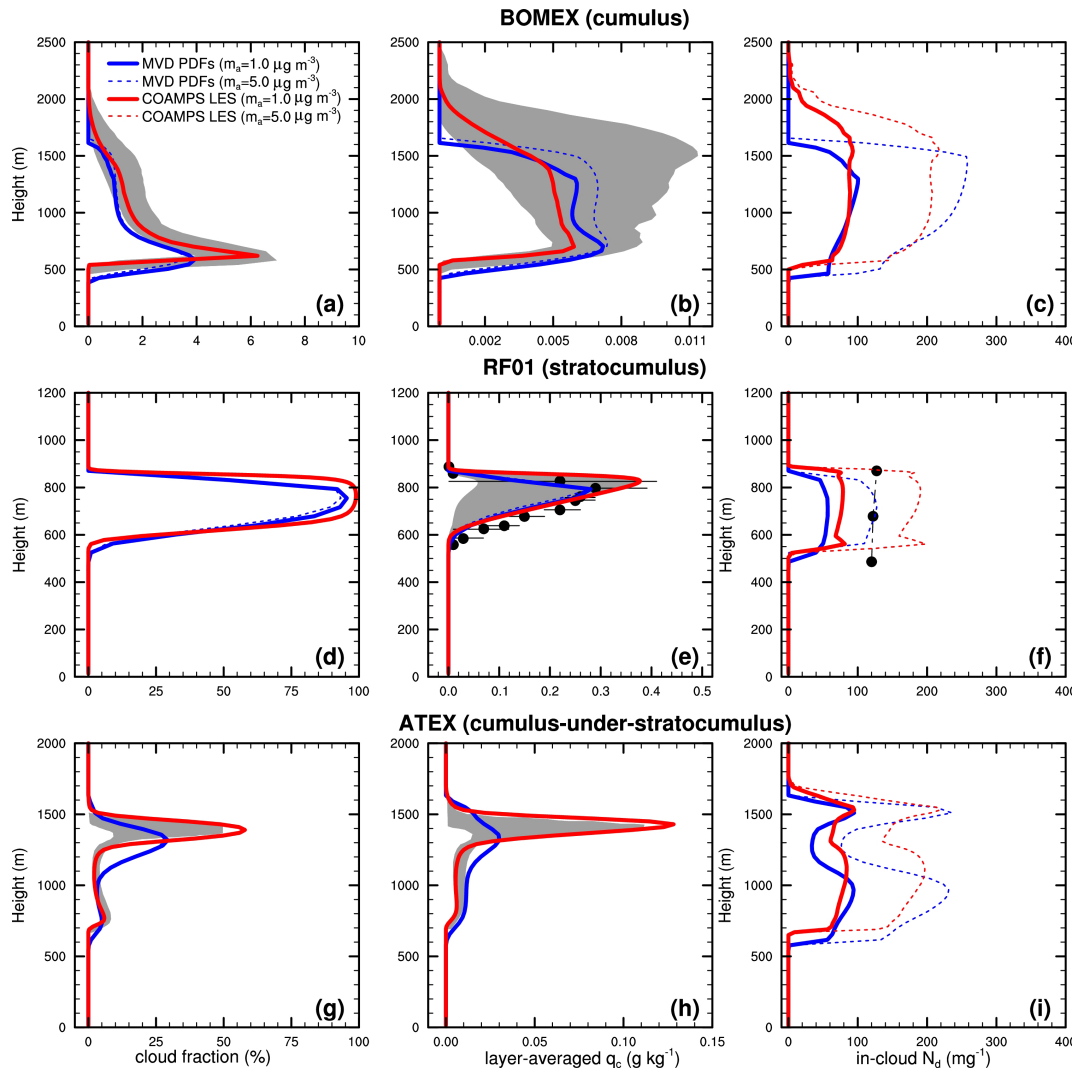


**Fig. 2.** Comparison of cloud fraction, layer-averaged cloud water content ( $q_c$ ), and in-cloud cloud droplet number concentration ( $N_d$ ) from the MVD PDFs (blue) and from COAMPS LES and S-S LES (red) at different sulfate concentrations ( $m_a$ ), averaged over the last 3 h for BOMEX, last 2 h for RF01, last 5 h for ATEX, last 5 h for RICO, and last 4 h for RF02, corresponding to the periods for LES in Siebesma et al. (2003), Stevens et al. (2005), Stevens et al. (2001), Stevens and Seifert (2008), and Ackerman et al. (2009), respectively. The red solid and dotted curves are overlapped in (a), (b), (d), (e), (g), and (h) because the microphysics was not considered in COAMPS LES following a protocol established by GCSS for non-precipitating clouds. Shaded areas indicate the upper and lower bounds of the LES ensemble. Dots in (e) indicate averages of observed  $q_c$ , with horizontal bars indicating the first and third quartiles of the observed values (Zhu et al., 2005). Dots in (f), (i), (o) indicate averages of observed  $N_d$  (vanZanten et al., 2005; Stevens and Seifert, 2008).

Our SCM-CLUBB simulations are subject to the same initial conditions and large-scale forcings as the LES models (Stevens et al., 2001, 2005; Siebesma et al., 2003; Stevens and Seifert, 2008; Ackerman et al., 2009). This allows for a careful evaluation of SCM simulations against the LES. Because the LES can explicitly resolve most energy-carrying eddies, they are often used as benchmark simulations. In this study, we use COAMPS<sup>1</sup> LES (Golaz et al., 2005), which is

derived from the COAMPS meso-scale model (Hodur, 1997). The COAMPS LES model has been modified to include an anelastic pressure solver and to add cloud droplet number concentration as a prognostic variable with the aerosol activation scheme developed by Ming et al. (2006). For RICO, we use the LES results in Stevens and Seifert (2008, hereafter referred to as S-S LES).

The size distribution for sulfate is

$$N(\ln D) = \frac{N_1}{(2\pi)^{1/2} \ln \sigma_1} \exp\left(-\frac{(\ln D - \ln D_{g,1})^2}{2 \ln^2 \sigma_1}\right)$$

<sup>1</sup>COAMPS is a registered trademark of the Naval Research Laboratory

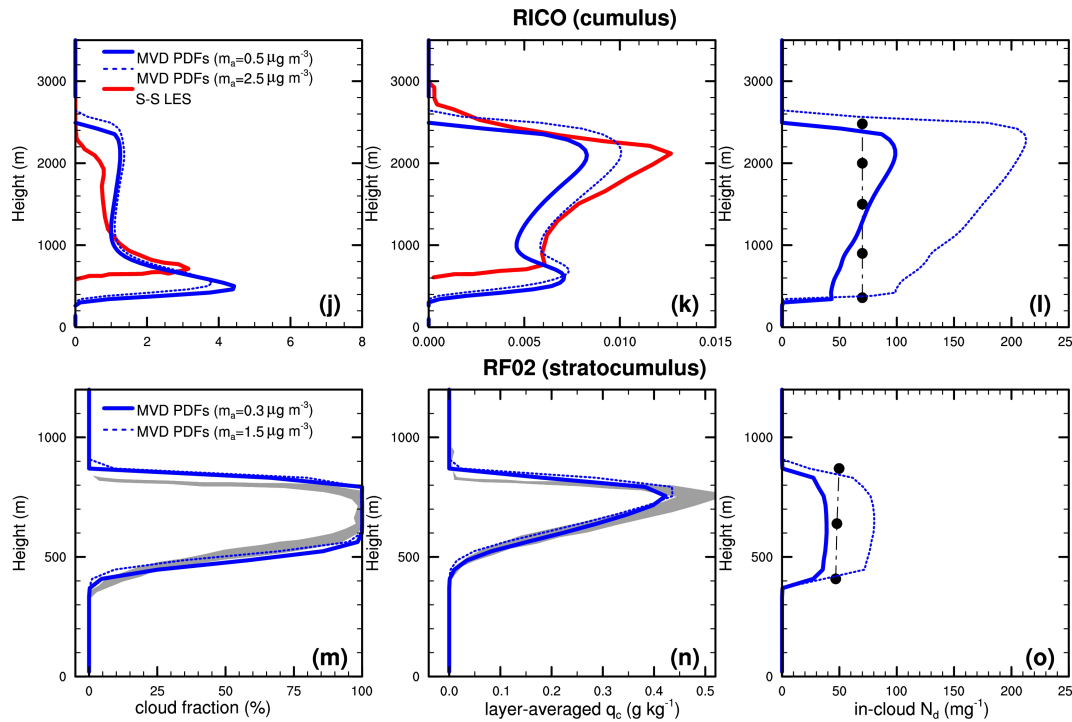


Fig. 2. Continued.

$$+ \frac{N_2}{(2\pi)^{1/2} \ln \sigma_2} \exp\left(-\frac{(\ln D - \ln D_{g,2})^2}{2 \ln^2 \sigma_2}\right)$$

where  $N_1 : N_2 = 17 : 3$ ,  $D_{g,1} = 0.01 \mu\text{m}$ ,  $\sigma_1 = 1.6$ ,  $D_{g,2} = 0.15 \mu\text{m}$ ,  $\sigma_2 = 2.0$ . To examine aerosol indirect effects, we present results using sulfate aerosol mass concentrations of  $1.0$  and  $5.0 \mu\text{g m}^{-3}$  for BOMEX, RF01, and ATEX;  $0.5$  and  $2.5 \mu\text{g m}^{-3}$  for RICO; and  $0.3$  and  $1.5 \mu\text{g m}^{-3}$  for RF02. For RF02,  $0.3 \mu\text{g m}^{-3}$  is obtained by integrating the sulfate size distribution in Ackerman et al. (2009). Specifying  $5.0$  and  $0.5 \mu\text{g m}^{-3}$  for RF01 and RICO, respectively, produces droplet number concentrations close to observed values (Fig. 2f and l). For droplet number, alternative parameterizations, including the diagnostic approach and the mechanistic approach with fixed vertical velocity variances, are examined and compared to the mechanistic approach with prognostic vertical velocity variances here.

CLUBB requires about an hour to spin-up PDFs of vertical velocity, which are critical for determining droplet number. Unrealistically low droplet numbers from unrealistically low vertical velocities during the spin-up period, distort all microphysical processes (e.g., precipitation) that depend on droplet number. Thus, the microphysics parameterization is not activated until one hour. In implementation in a free-standing large-scale model, this issue will not be relevant after model spin-up.

In the remainder of this section, we show simulations of liquid water path, cloud fraction, cloud droplet number concentrations, and vertical velocities using the GFDL SCM-

CLUBB, with aerosol activation and microphysics coupled as described in Sect. 2. Successful CLUBB simulations of cloud fraction and cloud liquid without aerosol activation or precipitation have been reported previously (Golaz et al., 2002b, 2007; Wyant et al., 2007). This section presents the first results on the effects of aerosols and precipitation on cloud fraction and cloud liquid using CLUBB and the first results on cloud droplet number concentrations obtained from CLUBB vertical velocities. In Sect. 3.3, we will contrast the MVD PDFs of vertical velocity with those using current state-of-the-science methods. Note that since the vertical velocity PDFs are crucial to the determination of cloud droplet number concentrations and precipitation, the results presented in Sects. 3.1 and 3.2 depend on vertical velocity PDFs.

### 3.1 Micro- and macrophysical properties

Liquid water paths (LWP) for all of the cases at both high and low aerosol concentrations fall within the ranges of LES in Stevens et al. (2001, 2005), Siebesma et al. (2003), Stevens and Seifert (2008), and Ackerman et al. (2009) (Fig. 1). Three cases observed to be non-precipitating produce very small surface precipitation rates in the GFDL SCM-CLUBB at high aerosol concentrations. These rates are at least an order of magnitude less than rates in the cases observed to be precipitating when aerosol concentrations are specified that yield droplet numbers close to observations (Table 1).



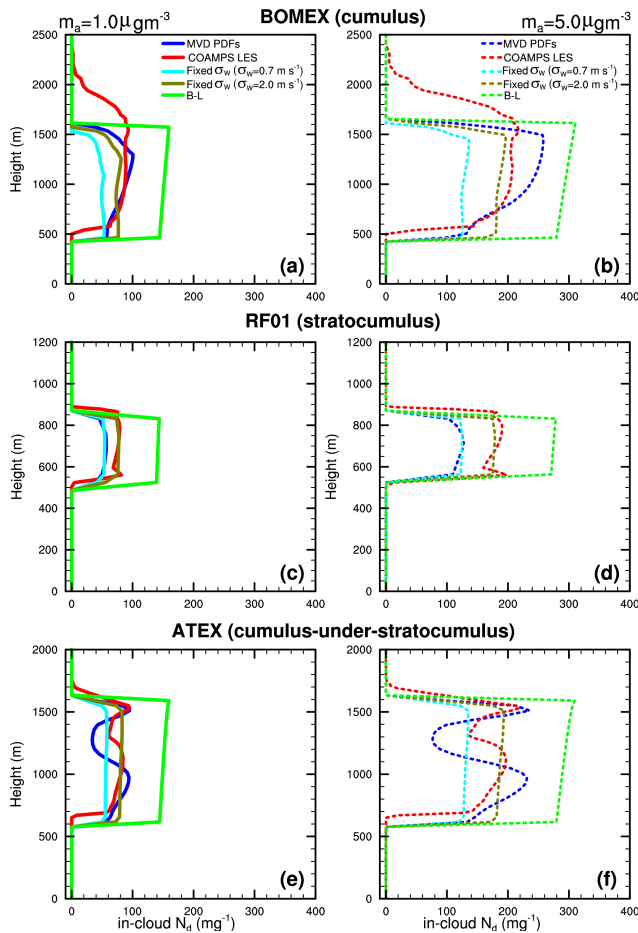


**Fig. 3.** Profiles of in-cloud droplet number concentrations ( $N_d$ ) at sulfate concentrations ( $m_a$ ) of  $1.0 \mu\text{g m}^{-3}$  in (a), (c), and (e), and of  $5.0 \mu\text{g m}^{-3}$  in (b), (d), and (f), averaged over the last 3 h for BOMEX in (a) and (b), last 2 h for RF01 in (c) and (d), and last 5 h for ATEX in (e) and (f).

Liquid water paths increase at high aerosol concentrations in the shallow cumulus cases BOMEX and RICO. The stratocumulus case, RF01, behaves differently, with slightly smaller liquid water paths at high aerosol concentrations. The liquid water path is also slightly smaller at high aerosol concentration in ATEX with both shallow cumulus and stratocumulus (Table 1). After case-dependent initial spin-up, the integrations are nearly steady. Some high-frequency oscillations are evident in RICO but only at low aerosol concentration.

These five cases are consistent with the range of responses to changing aerosol concentrations discussed in the scientific literature and show the potential utility of the MVD PDFs to discern different types of cloud-aerosol interactions. The shallow cumulus cases are consistent with the second aerosol indirect effect, in which increases in droplet number at high aerosol concentration inhibit precipitation, resulting in more cloud liquid (e.g., Albrecht, 1989). The stratocu-

**Table 1.** The surface precipitation rate (Precip. rate), liquid water path (LWP), and cloud optical depth ( $\tau$ ) at different sulfate aerosol mass concentrations ( $m_a$ ,  $\mu\text{g m}^{-3}$ ) from the GFDL SCM-CLUBB simulations.

	$m_a$ ( $\mu\text{g m}^{-3}$ )	Precip. rate ( $\text{mm day}^{-1}$ )	LWP ( $\text{g m}^{-2}$ )	$\tau$
BOMEX	1.0	0.11	6.2	0.8
	5.0	0.02	7.6	1.3
RF01	1.0	0.003	41.0	5.9
	5.0	0.0009	38.8	7.3
ATEX	1.0	0.002	14.1	2.3
	5.0	0.0004	13.9	3.1
RICO	0.5	0.21	11.4	1.3
	2.5	0.06	13.6	1.9
RF02	0.3	0.14	110.7	12.3
	1.5	0.05	110.3	15.3

Averages from the first hour (when the microphysics is activated) to the end of the simulations.

mulus cases exhibit behavior consistent with Ackerman et al. (2004) and Bretherton et al. (2007), in which increased evaporation of cloud liquid at high aerosol concentration acts to reduce cloud liquid. The latter mechanism is especially effective when the relative humidity above the inversion is low. The relative humidity above the inversion in RF01 is 10%.

More obviously, increased drop numbers and smaller drop size act to increase cloud optical depths ( $\tau$ ) through the first aerosol indirect effect (Table 1). As aerosol concentration  $m_a$  increases by a factor of 5, cloud albedo ( $\alpha_c$ ) increases from 0.43 to 0.49 for RF01, if we approximate  $\alpha_c$  as a function of  $\tau$ ,  $\alpha_c = \frac{\tau}{\tau + 7.7}$  for non-absorbing and homogeneous clouds, following Lacis and Hansen (1974).

Vertical profiles of cloud fraction and cloud liquid water generally agree well with LES and observations (Fig. 2). The vertical profiles are averaged over the last 3 h for BOMEX, last 2 h for RF01, last 5 h for ATEX, last 5 h for RICO, and last 4 h for RF02, corresponding to the periods for LES in Siebesma et al. (2003), Stevens et al. (2005, 2001), Stevens and Seifert (2008), and Ackerman et al. (2009), respectively, to which the GFDL SCM-CLUBB simulations are compared. The BOMEX, RF01, and ATEX LES follow a protocol established by GCSS for non-precipitating clouds and do not include microphysical processes (Stevens et al., 2001, 2005; Siebesma et al., 2003). In the absence of microphysics, the LES cloud fractions and liquid do not depend on aerosol concentration, since there are no mechanisms to remove cloud liquid. The Stevens and Seifert (2008) RICO LES include microphysics but with a prescribed drop number concentration ( $70 \text{ mg}^{-1}$ ). In BOMEX and RICO,

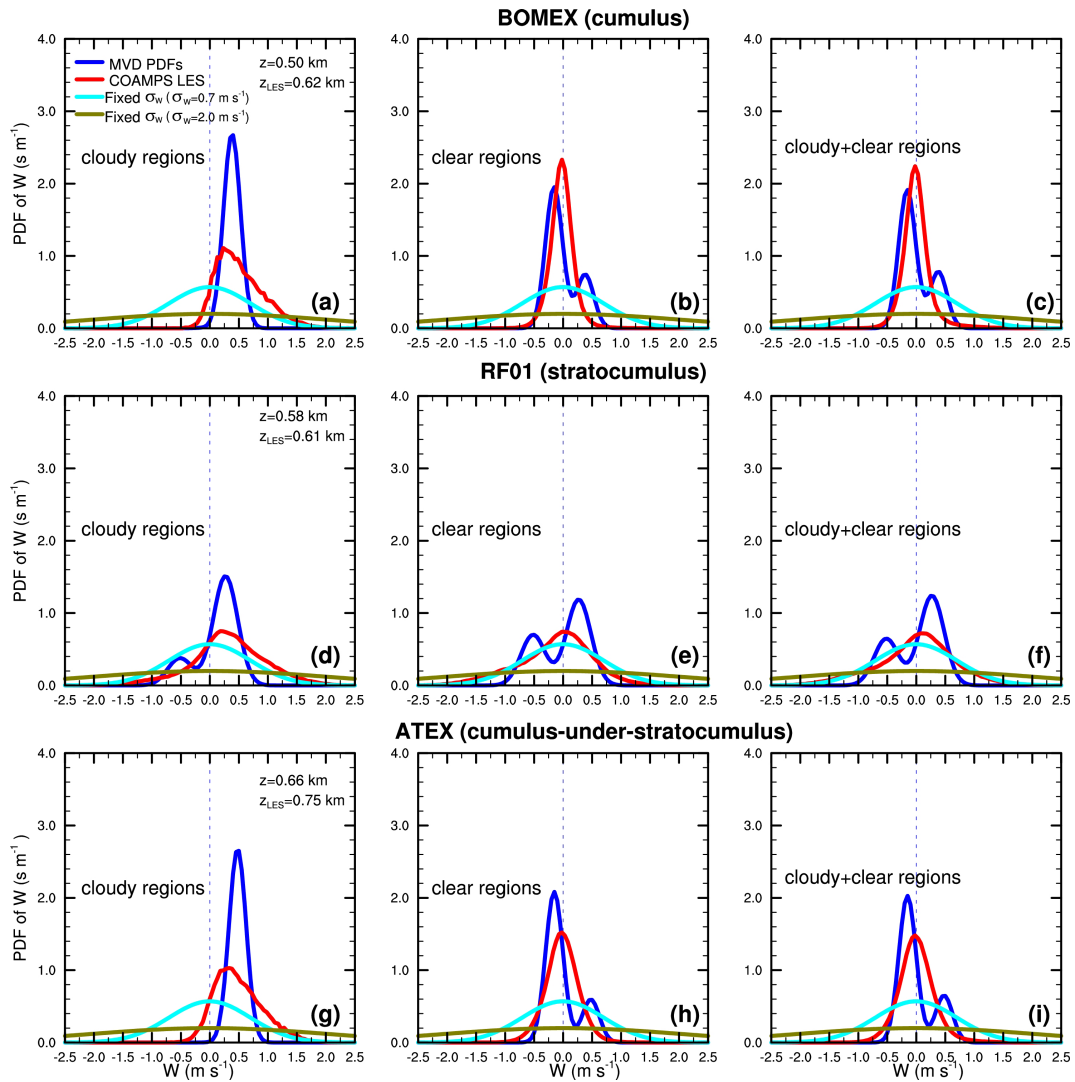


**Fig. 4.** Probability density function (PDF) of vertical velocity ( $w$ ) in cloudy regions, clear regions, and whole sky (cloudy + clear regions) averaged over the same periods as in Fig. 3, for BOMEX in (a), (b), and (c), RF01 in (d), (e), and (f), and ATEX in (g), (h), and (i).  $z$  and  $z_{LES}$  refer to the cloud base heights from the MVD PDFs and from COAMPS LES, respectively.

the MVD PDFs successfully reproduce trade-wind cumulus clouds with a small cloud fraction and layer-averaged liquid water content. In the RF01 and RF02 stratocumulus cases, the MVD PDFs simulate a shallow boundary layer and a solid cloud deck. In the cumulus-under-stratocumulus ATEX case, a cumulus layer is present from 600 m to 1100 m, and the cloud fraction increases to about 30% at cloud top.

This agreement is important, as it establishes the general credibility of the MVD PDFs and supports the argument that the PDFs of droplet number and vertical velocity, for which observations are not readily available, are also reasonable. Observations of drop numbers can be reproduced well by the MVD PDFs and LES for specified aerosol concentrations (Fig. 2f, l, and o).

### 3.2 Alternate parameterizations of droplet number

As discussed above, aerosols can exert significant impacts on cloud micro- and macrophysical properties by influencing the droplet concentration,  $N_d$ . We have also calculated  $N_d$  using two alternate methods that have been adopted in GCMs. One method retains a mechanistic approach but employs a simpler approach to generate the PDF of vertical velocity. The other uses a diagnostic relationship between aerosol concentration and  $N_d$  (Boucher and Lohmann, 1995).

In the first alternate method, the PDF of sub-grid vertical velocity is given by a single Gaussian distribution, whose width ( $\sigma_w$ ) is diagnosed either from turbulence kinetic energy (Lohmann et al., 1999) or from vertical eddy diffusivity (Morrison and Gettelman, 2008). A lower bound ( $\sigma_{min}$ ) is

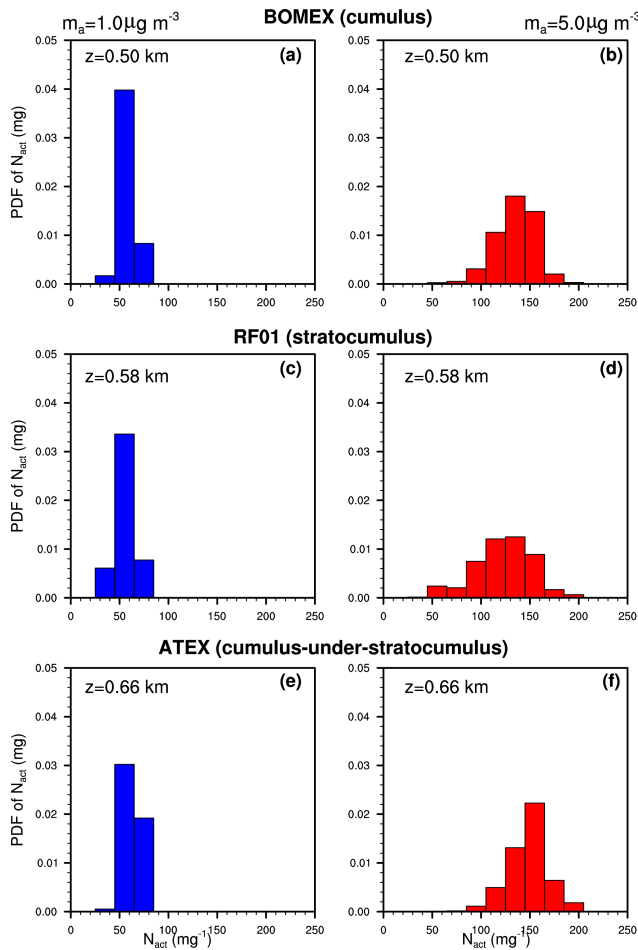


**Fig. 5.** Probability density function (PDF) of  $N_{\text{act}}$  at different sulfate concentrations ( $m_a$ ) near cloud bases averaged over the same periods as in Fig. 2 for BOMEX in (a) and (b), RF01 in (c) and (d), ATEX in (e) and (f), RICO in (g) and (h), and RF02 in (i) and (j).

usually imposed on  $\sigma_w$  and often dominates  $\sigma_w$ . We set  $\sigma_w$  to be  $\sigma_{\text{min}}$ , and set  $\sigma_{\text{min}}$  to be 0.7 or 2.0  $\text{m s}^{-1}$  in our sensitivity tests. The value of 0.7  $\text{m s}^{-1}$  is used in the GFDL AM3 (Donner et al., 2010). We hereafter refer to this alternate as fixed  $\sigma_w$ . The second alternate method uses an empirical relationship between  $N_d$  and the sulfate mass concentration following Boucher and Lohmann (1995), hereafter referred to as B-L.

The profiles of the in-cloud droplet number concentration averaged over the last 3 h for BOMEX, last 2 h for RF01, and last 5 h for ATEX are presented in Fig. 3. With the increase of  $m_a$  by a factor of 5,  $N_d$  is enhanced by a factor of  $\sim 2$ , indicating the greater competition for water at a higher  $m_a$ . The in-cloud  $N_d$  is almost constant with height in the sensitivity tests of fixed  $\sigma_w$  and B-L, mainly because  $m_a$  and  $\sigma_w$  are constant with height. Compared to the COAMPS LES results, the sensitivity tests of fixed  $\sigma_w$  with  $\sigma_w = 0.7 \text{ m s}^{-1}$  underestimate  $N_d$ . This underestimation can be alleviated

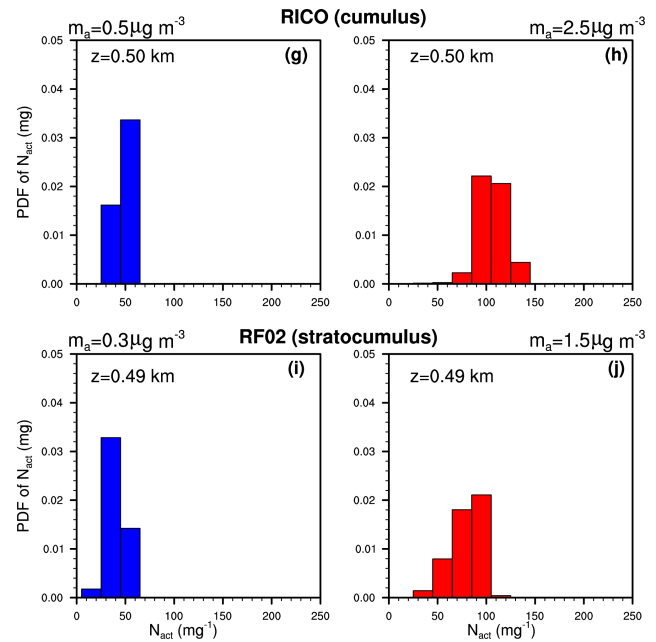


**Fig. 5.** Continued.

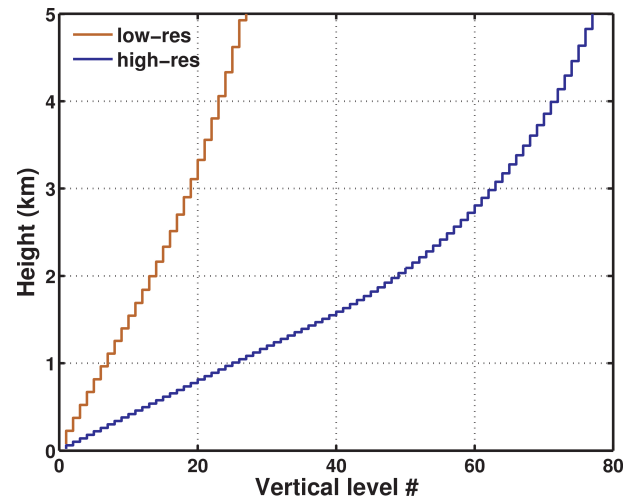


**Fig. A1.** Vertical distribution of grid levels for the GFDL SCM-CLUBB using the multi-variate probability density functions with dynamics (MVD PDFs) at lower (brown) and higher (blue) resolutions.

by enhancing  $\sigma_w$ . When  $\sigma_w$  is enhanced to 2.0  $\text{m s}^{-1}$ ,  $N_d$  agrees well with the LES results. The tests of B-L overestimate  $N_d$ . This overestimation has also been found by other model studies (Ghan et al., 1997). Although using a fixed  $\sigma_w$  of 2.0  $\text{m s}^{-1}$  produces good agreement with LES, such a large value is greater than that commonly used in GCMs (from 0.25 to 0.75  $\text{m s}^{-1}$  in Chuang et al., 1997; 0.1  $\text{m s}^{-1}$  in Ghan et al., 1997; 0.7  $\text{m s}^{-1}$  in Donner et al., 2010).



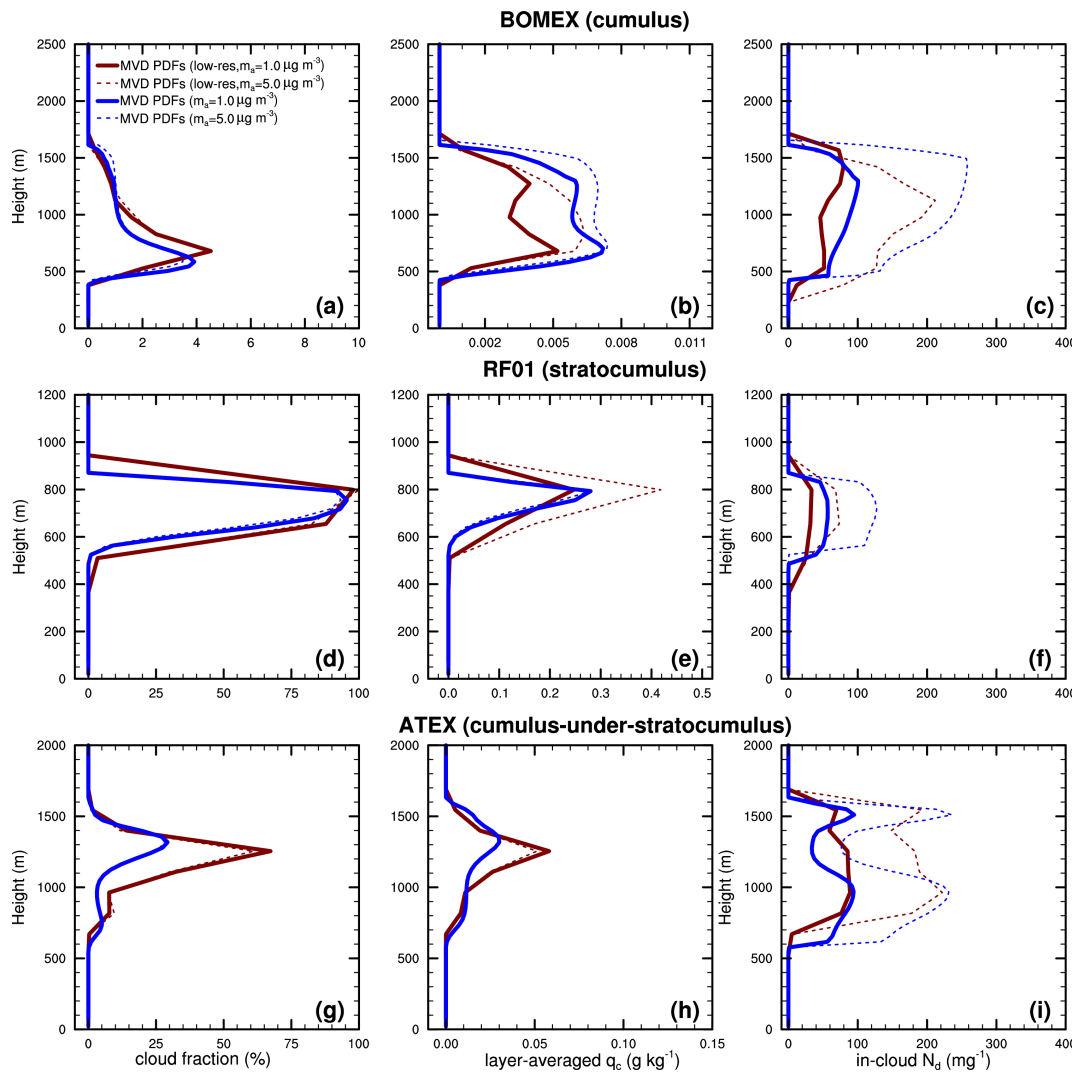


Fig. A2. Similar to Fig. 2 but at different resolutions.

### 3.3 PDFs of $w$ and $N_{act}$

Sub-grid variability of vertical velocity is critical for aerosol activation. To illustrate this variability, we show the PDF of the vertical velocity ( $w$ ) around the level of cloud base in cloudy regions, clear regions, and whole sky (Fig. 4).

Aerosol activation is controlled by the PDF of  $w$  in cloudy regions. The mean vertical velocity is positive in cloudy regions in both the MVD PDFs and the COAMPS LES, but not in clear regions. The different features of  $w$  between cloudy and clear regions show that  $w$  is correlated with temperature and moisture. Over the whole sky (cloudy + clear regions),  $w$  is positively skewed in BOMEX (Fig. 4c). The positive skewness is characteristic of cumulus clouds, with updraft cores surrounded by a large area of weak downdrafts (LeMone, 1989; Moeng and Rotunno, 1990). A single Gaus-

sion distribution is unable to represent the skewness. PDFs from aircraft data have shown that some PDFs are correlated and skewed (Larson et al., 2002).

Regardless of specified variance, the fixed-variance  $\sigma_w$  distribution differs strongly from both the LES distributions and the MVD PDFs in clear and cloudy regions. The MVD PDFs with a single peak tend to be narrower than the LES distributions (Fig. 4a and g), and the MVD PDFs of comparable width to the LES distributions are characterized by secondary peaks. The MVD PDFs and LES distributions agree substantially better than the fixed-variance and LES distributions do.

Also evident in Fig. 4 is the reason for the good agreement of  $N_d$  between the LES and the fixed variance ( $\sigma_w$ ) of  $2.0 \text{ m s}^{-1}$ . The  $w$  PDF for this value differs appreciably from the LES distribution. Two discrepant features in the

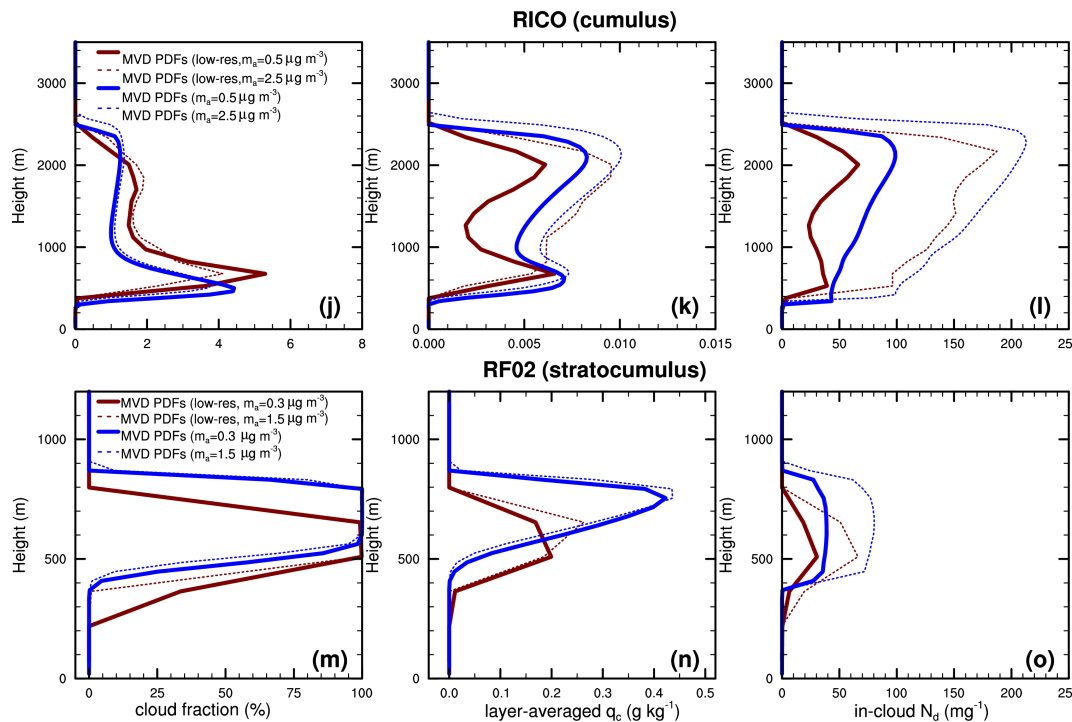


Fig. A2. Continued.

fixed-variance distribution compensate each other. The fat tail of positive updrafts allows more activation than the LES distribution, but its zero mean allows less.

To illustrate the impact of the sub-grid variability of the vertical velocity on aerosol activation, we show the PDF of the activated droplet number concentration  $N_{\text{act}}$  near cloud bases (Fig. 5). As expected, for a smaller  $m_a$ ,  $N_{\text{act}}$  peaks around a smaller value. For example,  $N_{\text{act}}$  peaks around 35 and  $150 \text{ mg}^{-1}$  for  $m_a = 0.3$  and  $5.0 \mu\text{g m}^{-3}$ , respectively. The PDFs of  $N_{\text{act}}$  illustrate that droplets are not uniformly distributed. Although we do not do so, these PDFs could be used in microphysics and radiative transfer to take the sub-grid variability of droplet concentrations into account using sub-columns for different members of the PDF of  $N_d$  (Pincus et al., 2006), or sampling (Larson et al., 2005).

#### 4 Conclusions

Results using MVD PDFs of moisture, temperature, and vertical velocity to parameterize cloud fraction, condensate, and droplet number concentration are promising. We have examined five representative cloud cases, which span many moist boundary layer regimes. The cloud profiles from the MVD PDFs agree well with those from LES and available observations. This good agreement has been achieved without any case-specific adjustments. The uniform treatment of the planetary boundary layer should benefit global simulations where a variety of regimes exist. Moreover, for the first time,

the successful simulation of cloud droplet number concentration from the MVD PDFs has been achieved.

With the coupling to a two-moment microphysics, the predicted droplet number concentration is allowed to influence cloud microphysics. As aerosol mass concentration increases, droplet concentration increases and precipitation decreases. Liquid water path can either increase or decrease, consistent with established conceptual models and LES. Vertical velocities produced by the MVD PDFs successfully capture the skewed character frequently associated with boundary layers.

An especially powerful result from the MVD PDFs is the range of cloud-aerosol interactions it supports, including changes in liquid water path of both signs as aerosol concentrations increase. Successful simulations of aerosol indirect effects in climate models will require parameterizations that capture this full range of interactions, of correct quantitative magnitude and association with boundary-layer regimes. It is now crucial to evaluate the behavior of the MVD PDFs using LES including both activation and full microphysics, rather than the more limited LES available for this study. The Ackerman et al. (2004) and Bretherton et al. (2007) studies are suggestive but should be followed up by quantitative case-specific comparisons. It is also very important to augment GCSS case studies with observations of aerosols and vertical velocities.

## Appendix A

### Lower-resolution SCM-CLUBB simulations

To explore the consequence of lower vertical resolution, we have conducted lower resolution simulations with 67 vertical levels and vertical spacing of  $\sim 150$  m in the lowest 2 km (Fig. A1). The vertical levels for the MVD PDFs and for the host SCM coincide. The time steps are 5 min and 30 min for the MVD PDFs and the host SCM, respectively.

Figure A2 shows the cloud profiles of five representative cases using different resolutions. In many cases, the lower and higher resolution results are qualitatively similar, though less so for cases observed to be precipitating. For BOMEX, RF01, and RICO, the cloud fraction and cloud water content agree well between the lower and higher resolution simulations. For ATEX, cloud fraction is over-predicted, and two cloud layers are less distinct. For RF02, the cloud layers at lower resolution are lower with less cloud liquid. Systematically, drop numbers are lower, evidently the result of degraded vertical velocity PDFs at lower resolution.

Although the lower resolution SCM-CLUBB simulations are not quantitatively as accurate as the higher resolution simulations, they, nonetheless, are able to capture the major properties of cumulus and stratocumulus regimes. When implementing the MVD PDFs in large-scale models, reduced accuracy at lower resolution would be balanced against computational cost. It is difficult based on the SCM cases to yet assess the necessary resolution for the MVD PDFs in large-scale models.

*Acknowledgements.* H. Guo is supported by the grant GC08-249, Climate Prediction Program for the Americas (CPPA), NOAA Climate Program Office. V. E. Larson, D. P. Schanen, and B. M. Griffin acknowledge support by grant ATM-0936186 from the National Science Foundation and by grant NA09OAR4310123 from NOAA.

Edited by: O. Boucher

### References

- Ackerman, A. S., Kirkpatrick, M. P., Stevens, D. E., and Toon, O. B.: The impact of humidity above stratiform clouds on indirect aerosol climate forcing, *Nature*, 432, 1014–1017, 2004.
- Ackerman, A. S., VanZanten, M. C., Stevens, B., et al.: Large-eddy simulations of a drizzling, stratocumulus-topped marine boundary layer, *Mon. Weather Rev.*, 137, 1083–1110, 2009.
- Albrecht, B. A.: Aerosols, cloud microphysics, and fractional cloudiness, *Science*, 243, 1227–1230, 1989.
- Boucher, O. and Lohmann, U.: The sulfate-CCN-cloud albedo effect: A sensitivity study with two general circulation models, *TELLUS*, 47B, 281–300, 1995.
- Bretherton, C. S., Blossey, P. N., and Uchida, J.: Cloud droplet sedimentation, entrainment efficiency, and subtropical stratocumulus albedo, *Geophys. Res. Lett.*, 34, L03813, doi:10.1029/2006GL027648, 2007.
- Chuang, C. C., Penner, J. E., Taylor, K. E., Grossman, A. S., and Walton, J. J.: An assessment of the radiative effects of anthropogenic sulfate, *J. Geophys. Res.*, 102(D3), 3761–3778, 1997.
- Donner, L. J., Seman, C. J., and Hemler, R. S.: Three-dimensional cloud-system modeling of GATE convection, *J. Atmos. Sci.*, 56, 1885–1912, 1999.
- Donner, L. J., Wyman, B. L., Hemler, R. S., et al.: The dynamical core, physical parameterizations, and basic simulation characteristics of the atmospheric component of the GFDL global coupled model CM3, *J. Climate*, submitted, 2010.
- Forster, P., Ramaswamy, V., Artaxo, P., et al.: Changes in Atmospheric Constituents and in Radiative Forcing, in: *Climate Change 2007: The Physical Science Basis, Contribution of Working Group I to the Fourth Assessment Report of the Intergovernmental Panel on Climate Change*, edited by: Solomon, S., Qin, D., Manning, M., Chen, Z., Marquis, M., Averyt, K. B., Tignor, M., and Miller, H. L., Cambridge University Press, Cambridge, United Kingdom and New York, NY, USA, 2007.
- Ghan, S. J., Leung, L. R., Easter, R. C., and Abdul-Razzak, H.: Prediction of cloud droplet number in a general circulation model, *J. Geophys. Res.*, 102, 21777–21794, 1997.
- Golaz, J.-C., Larson, V. E., and Cotton, W. R.: A PDF based model for boundary layer clouds. Part I: Method and model description, *J. Atmos. Sci.*, 59, 3540–3551, 2002a.
- Golaz, J.-C., Larson, V. E., and Cotton, W. R.: A PDF based model for boundary layer clouds. Part II: Model results, *J. Atmos. Sci.*, 59, 3552–3571, 2002b.
- Golaz, J.-C., Wang, S., Doyle, J. D., and Schmidt, J. M.: COAMPS<sup>®</sup>-LES: Model evaluation and analysis of second and third moment vertical velocity budgets, *Bound.-Layer Meteorol.*, 116, 487–517, 2005.
- Golaz, J.-C., Larson, V. E., Hansen, J. A., Schanen, D. P., and Griffin, B. M.: Elucidating model inadequacies in a cloud parameterization by use of an ensemble-based calibration framework, *Mon. Weather Rev.*, 135, 4077–4096, 2007.
- Heintzenberg, J. and Charlson, R. J.: *Clouds in the perturbed climate system*, MIT press, 2009.
- Hodur, R. M.: The Naval Research Laboratory's Coupled Ocean/Atmosphere Mesoscale Prediction System (COAMPS), *Mon. Weather Rev.*, 125, 1414–1430, 1997.
- Kiehl, J. T.: Twentieth century climate model response and climate sensitivity, *Geophys. Res. Lett.*, 34, L22710, doi:10.1029/2007GL031383, 2007.
- Lacis, A. A. and Hansen, J. E.: A parameterization for the absorption of solar radiation in the earth's atmosphere, *J. Atmos. Sci.*, 31, 118–133, 1974.
- Lappen, C.-L. and Randall, D. A.: Toward a unified parameterization of the boundary layer and moist convection. Part I: A new type of mass-flux model, *J. Atmos. Sci.*, 58, 2021–2036, 2001.
- Larson, V.-E, Golaz, J.-C., and Cotton, W. R.: Small-scale and mesoscale variability in cloudy boundary layers: Joint probability density function, *J. Atmos. Sci.*, 59, 3519–3539, 2002.
- Larson, V. E. and Golaz, J.-C.: Using probability density functions to derive consistent closure relationships among higher-order moments, *Mon. Weather Rev.*, 133, 1023–1042, 2005.
- Larson, V. E, Golaz, J.-C., Jiang, H., and Cotton, W. R.: Supplying local microphysics parameterizations with information about subgrid variability: Latin Hypercube Sampling, *J. Atmos. Sci.*, 62, 4010–4026, 2005.

- Leary, C. A. and Houze Jr., R. A.: The contribution of mesoscale motions to the mass and heat fluxes of an intense tropical convective system, *J. Atmos. Sci.*, 37, 784–796, 1980.
- LeMone, M. A.: Some observations of vertical velocity skewness in the convective planetary boundary layer, *J. Atmos. Sci.*, 47, 1163–1169, 1989.
- Lohmann, U., Feichter, J., Chuang, C. C., and Penner, J. E.: Prediction of the number of cloud droplets in the ECHAM GCM, *J. Geophys. Res.*, 104, 9169–9198, 1999.
- Mellor, G. L.: The Gaussian cloud model relations, *J. Atmos. Sci.*, 34, 356–358, 1977.
- Moeng, C.-H. and Rotunno, R.: Vertical-velocity skewness in the buoyancy-driven boundary layer, *J. Atmos. Sci.*, 47, 1149–1162, 1990.
- Ming, Y., Ramaswamy, V., Donner, L. J., and Phillips, V. T. J.: A new parameterization of cloud droplet activation applicable to General Circulation Models, *J. Atmos. Sci.*, 63, 1348–1356, 2006.
- Ming, Y., Ramaswamy, V., Donner, L. J., Phillips, V. T. J., Klein, S. A., Ginoux, P. A., and Horowitz, L. W.: Modeling the interactions between aerosol and liquid water clouds with a self-consistent cloud scheme in a General Circulation Model, *J. Atmos. Sci.*, 64, 1189–1209, 2007.
- Morrison, H. and Gettelman, A.: A new two-moment bulk stratiform cloud microphysics scheme in the Community Atmosphere Model, Version 3 (CAM3). Part I: Description and numerical tests, *J. Climate*, 21, 3642–3659, 2008.
- Ovtchinnikov, M. and Ghan, S. J.: Parallel simulations of aerosol influence on clouds using cloud-resolving and single-column models, *J. Geophys. Res.*, 110, D15S10, doi:10.1029/2004JD005088, 2005.
- Pincus, R., Hemler, R. S., and Klein, S. A.: Using stochastically generated sub-columns to represent cloud structure in a large-scale model, *Mon. Weather Rev.*, 134, 3644–3656, 2006.
- Randall, D. A., Xu, K. M., Somerville, R. J. C., and Iacobellis, S.: Single-column models and cloud ensemble models as links between observations and climate models, *J. Climate*, 9, 1683–1697, 1996.
- Salzmann, M., Ming, Y., Golaz, J.-C., Ginoux, P. A., Morrison, H., Gettelman, A., Krämer, M., and Donner, L. J.: Two-moment bulk stratiform cloud microphysics in the GFDL AM3 GCM: description, evaluation, and sensitivity tests, *Atmos. Chem. Phys.*, 10, 8037–8064, doi:10.5194/acp-10-8037-2010, 2010.
- Siebesma, A. P., Bretherton, C. S., Brown, A., et al.: A large-eddy simulation intercomparison study of shallow cumulus convection, *J. Atmos. Sci.*, 60, 1201–1219, 2003.
- Stevens, B., Feingold, G., Cotton, W. R., and Walko, R. L.: Elements of the microphysical structure of numerically simulated non-precipitating stratocumulus, *J. Atmos. Sci.*, 53, 980–1006, 1996.
- Stevens, B., Ackerman, A. S., Albrecht, B. A., et al.: Simulations of trade-wind cumuli under a strong inversion, *J. Atmos. Sci.*, 58, 1870–1891, 2001.
- Stevens, B., Lenschow, D. H., Vali, G., et al.: Dynamics and chemistry of marine stratocumulus-DYCOMS-II, *B. Am. Meteorol. Soc.*, 84, 579–593, 2003.
- Stevens, B., Moeng, C.-H., Ackerman, A. S., et al.: Evaluation of large-eddy simulations via observations of nocturnal marine stratocumulus, *Mon. Weather Rev.*, 133, 1443–1462, 2005.
- Stevens, B. and Seifert, A.: Understanding macrophysical outcomes of microphysical choices in simulations of shallow cumulus convection, *J. Meteor. Soc. Japan*, 86A, 143–162, 2008.
- vanZanten, M. C., Stevens, B., Vali, G., and Lenschow, D.: Observations of drizzle in nocturnal marine stratocumulus, *J. Atmos. Sci.*, 62, 88–106, 2005.
- Webb, M. J., Senior, C. A., Sexton, D. M. H., et al.: On the contribution of local feedback mechanisms to the range of climate sensitivity in two GCM ensembles, *Clim. Dynam.*, 27, 17–38, 2006.
- Wyant, M. C., Bretherton, C. B., Chlond, A., et al.: A single-column model intercomparison of a heavily drizzling stratocumulus-topped boundary layer, *J. Geophys. Res.*, 112, D24204, doi:10.1029/2007JD008536, 2007.
- Zhu, P., Bretherton, C. S., Köhler, M., et al.: Intercomparison and interpretation of single column model simulations of a nocturnal stratocumulus topped marine boundary layer, *Mon. Weather Rev.*, 133, 2741–2758, 2005.